

# Growth and thermal properties change of CRUD deposited on fuel cladding in PWR power plant

Yunju Lee, Junhyuk Ham, Seung Chang Yoo, Dae Hyeon Park, Ji Hyun Kim\*

Department of Nuclear Engineering, College of Engineering, Ulsan National Institute of Science and Technology (UNIST)

\*Corresponding author: kimjh@unist.ac.kr

## 1. Introduction

In nuclear power plants, corrosion product related deposit (crud) is formed by sub-cooled boiling on the upper part of fuel cladding.[1-3] The corrosion products provoke serious economics and safety issues, which related with boron accumulation and radioactivation of itself. The crud deposition and boron accumulation are influenced by chemical and thermal-hydraulic behavior of water near fuel cladding surface.[4,5] Thus, to predict the crud deposition, crud deposition mechanism should be investigated considering chemical and thermal-hydraulic condition.[1,2,5] While crud thickness is known to be dependent on deposition time, there is no detail study conducted investigate the morphology changes of crud with different deposition time.[1,2,6]

In this study, to investigate morphology change of crud on fuel cladding, crud deposition experiment was conducted for three different periods in simulated primary water of pressurized water reactor (PWR). The specimens were examined by optical microscopy, scanning electron microscopy with focused ion beam instrument and energy dispersive X-ray spectroscopy. To investigate the effect of crud morphology on its thermal properties, thermal conductivity of crud was calculated from cladding wall temperature difference before and after the crud deposition experiment.

## 2. Experimental Methods

### 2.1. Experimental condition

To simulate the CRUD deposition at reactor core, three major conditions should be satisfied: existence of corrosion product in the primary water, sub-cooled boiling at cladding surface, and dissolved boron and lithium species in the primary water. To investigate the growth mechanism of CRUD, three experiment was conducted for 1day (T-1d), 3 days (T-3d) and 7 days (T-7d) each.

For in-situ surface temperature measurement, a thermocouple is spot welded at inner surface of the specimen. The test section autoclave is located at test section loop so that high pressure, high temperature and high flow rate conditions were constructed. The cladding specimen was installed at test section autoclave and penetrating the autoclave by using feedthrough fitting so that the specimen can be connected to electrode.

Table 1 Experimental conditions of crud deposition experiment

	T-1d	T-3d	T-7d
Exposure time [days]	1	3	7
Specimen Surface Temp.[°C]	352.8	356.0	354.9
Bulk Coolant Temp.[°C]	322	323	320
Pressure [bar]		155	
Saturation Temp. [°C]		345	
Specimen Heat Flux[kW/m <sup>2</sup> ]		67.0	
DO [ppb]		~<5	
DH [cc/kg]		25	
B [ppm]		1200	
Li [ppm]		2.2	
Ni [ppm]		25.0	
Fe [ppm]		12.0	

### 2.2. Analysis strategy

After a brief visual inspection, microscopic observation was conducted with FIB-SEM instrument. To investigate the axial characteristic of the CRUD, the specimen is cut in three pieces in axial direction (Top, Middle, Bottom) and SEM was conducted for each specimen. In this paper, analysis result of top region (270 mm from bottom) in each would be compared and discussed.

During experiment, cladding surface temperature was increased after metal ion injection. This indicate that crud layer, which can be act as heat transfer resistance, is formed. In this paper, effective thermal conductivity of crud was calculated from temperature difference before and after the crud formation. By assuming that bulk coolant temperature and convective heat transfer coefficient of cladding/coolant interface or crud/coolant interface is equal before and after crud deposition, effective thermal conductivity could be calculated by Equation 1.

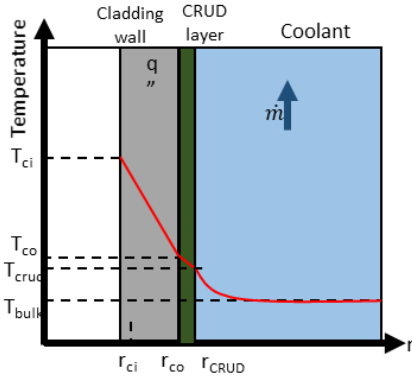


**Figure 1.** Schematic diagram of temperature change near cladding wall.

$$k_{Crud} = \frac{\frac{q'' \pi D_{oxide}}{4A_{cross,cl}} \left[ 2r_{oxide}^2 \ln\left(\frac{r_{oxide}}{r_{Crud}}\right) + (r_{Crud}^2 - r_{oxide}^2) \right]}{(T_{ci,f} - T_{ci,t}) - \frac{q'' \pi D_{co}}{A_{cross,cl}} \frac{1}{4k_{oxide}} \left[ 2r_{co}^2 \ln\left(\frac{r_{co}}{r_{oxide}}\right) + (r_{oxide}^2 - r_{co}^2) \right]} \quad (1)$$

### 3. Results and discussion

#### 3.1. Structural and chemical analysis of crud layer

From surface image of each specimen, dense layer composed of nanometer size particles is observed on the top of CRUD layer in all specimens. In the dense layer a few of chimney structures were observed. Chimney diameter distributed from 5~20  $\mu\text{m}$  and do not show any markable difference between each specimen.

From cross sectional SEM images of each specimen (Figure 2), dense layer which composed of nanometer sized equiaxed particles was also observed on top of CRUD layer. EDS analysis results of dense layer are clearly distinct with under CRUD layer. The dense layer is unexpected deposit formed from temperature change, which occurred on shut-down period. In this paper, CRUD layer which deposited on purposed experimental time was analyzed only.

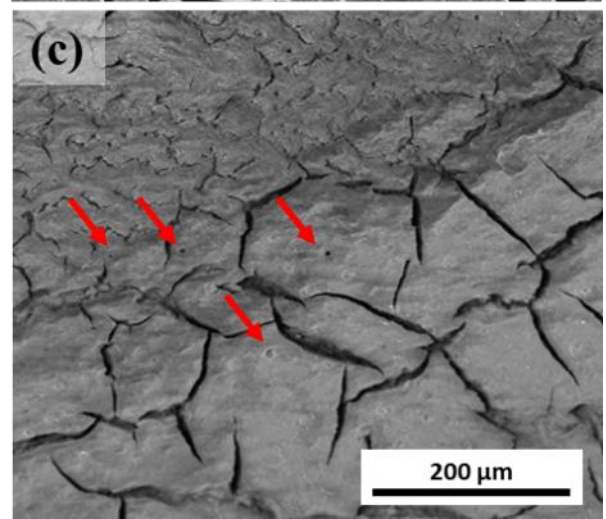
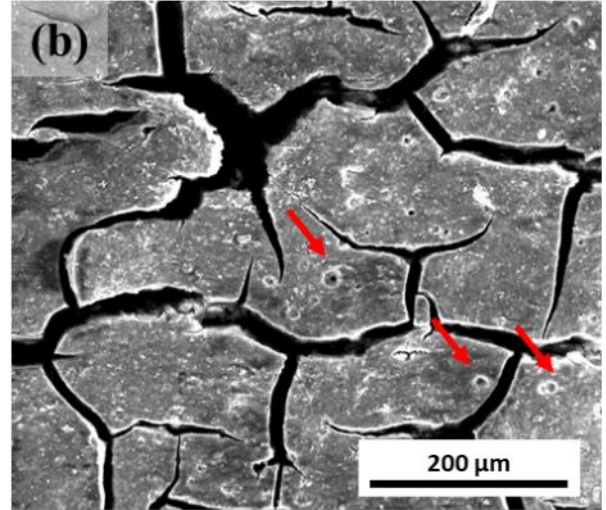
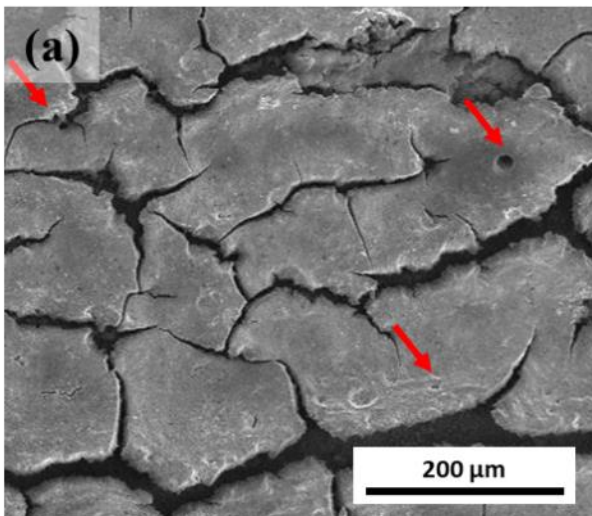


**Figure 2** Surface SEM image of CRUD layer which deposited on (a) T-1d, (b) T-3d and T-7d specimen

In T-1d specimen equiaxed particles are usually deposited while CRUD layer deposited on T-3d and T-7d specimens are mainly composed of needle-like structure of petal-like structures. From EDS analysis, it was found that needle-like or petal-like structure are composed of nickel oxide and equiaxed particles are usually composed of nickel ferrite.

Characteristics of CRUD layer deposited on each specimen were summarized on Table 2. As expected, thickness and Ni/Fe ratio of CRUD were increased as deposition time increased. Ni/Fe ratio increased dramatically between 1 to 3 days and increasing rate was decreased after 3 days. Surface temperature change of cladding after CRUD deposition was also increased with deposition time. However, thermal conductivity of CRUD increased between 1 to 3 days.

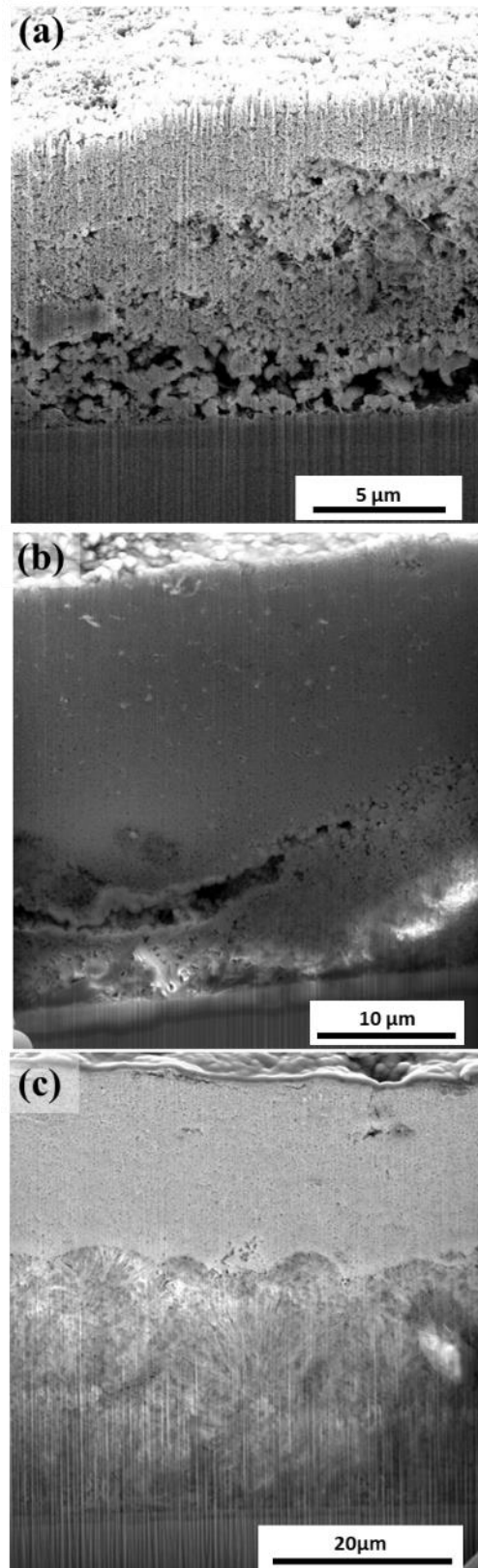


**Figure 3** Cross sectional image of CRUD layer which deposited on (a)T-1d, (b)T-3d, (c)T-7d specimen.

**Table 2** Structural and chemical characteristics of CRUD layer

	1 day	3 day	7 day
Thickness of Zr oxide layer	1.72 $\mu\text{m}$	2.95 $\mu\text{m}$	1.38 $\mu\text{m}$
Thickness of CRUD	4.96 $\mu\text{m}$	11.1 $\mu\text{m}$	26.0 $\mu\text{m}$
Average Ni/Fe ratio of CRUD	1.1	6.0	7.3

This can be explained by chemical composition of CRUD layer. Because formation of nickel ferrite particle is spontaneous and preferred than nickel oxide needles in PWR primary water chemistry, nickel ferrite particles are mainly deposited in early stage. From previous study, which summarized numerous analysis results of PWR fuel cladding CRUD, it was found that needle-like nickel oxide are deposited on cladding surface which were exposed to more severe temperature condition.[7] As the CRUD layer grows, cladding surface temperature increases and needle-like nickel oxide formation also increased. Because nickel oxide has higher thermal conductivity than nickel ferrite, thermal conductivity of CRUD also increased. From 3 to 7 days, thermal conductivity of CRUD decreased due to growth of CRUD layer.

**Table 3** Cladding surface temperature change and calculated thermal conductivity of CRUD layer

	1 day	3 day	7 day
Cladding surface temperature change after Crud deposition	1.8 $^{\circ}\text{C}$	2.0 $^{\circ}\text{C}$	2.5 $^{\circ}\text{C}$
Calculated thermal conductivity	1.1 mW/m-K	3.8 mW/m-K	0.68 mW/m-K

#### 4. Conclusions

To investigate the growth mechanism of CRUD, simulated CRUD deposition experiment was conducted for different time. As deposition time increased needle-like or petal-like nickel oxide are formed dominantly. Ni/Fe ratio increased dramatically between 1 to 3 days and increasing rate was decreased after 3 days. Although, both CRUD thickness and the temperature difference of cladding increased as time increased, thermal conductivity of CRUD decreased before 3 days. The thermal conductivity change can be explained by increase of nickel oxide, which have relatively high thermal conductivity than nickel ferrite.

## **ACKNOWLEDGEMENT**

This work was supported by the Nuclear Safety Research Program through the Korea Foundation Of Nuclear Safety (KoFONS) using the financial resource granted by the Nuclear Safety and Security Commission (NSSC) of the Republic of Korea. (No. 2106022) This study contains the results obtained by using the equipment of UNIST Central Research Facilities (UCRF).

## **REFERENCES**

- [1] T. Alhashan, M. Elforjani, A. Addali, J. Teixeria, Monitoring of bubble formation during the boiling process using acoustic emission signals, *Int. J. Eng. Res. Sci.* 2(4), 66-72, 2016.
- [2] S. H. Baek, H. -S. Shim, J. G. Kim, D. H. Hur, Visualization and acoustic emission monitoring of nucleate boiling on rough and smooth fuel cladding surfaces at atmospheric pressure, *Nucl. Eng. Des.*, 330, 429-436, 2018.
- [3] C. A. Brett, A. O. Brett, *Electrochemistry*, Oxford Univ. Press, New York, 1994.
- [4] J. Deshon, *Simulated Fuel Crud Thermal Conductivity Measurements Under Pressurized Water Reactor Conditions*, TR-1022896, EPRI, Palo Alto, CA.
- [5] D. Hussey, *PWR Axial Offset Anomaly (AOA) Guidelines*, TR-1008102, EPRI, Palo Alto, CA.
- [7] EPRI report (2004) *Evaluation of Fuel Clad Corrosion Product Deposits and Circulating Corrosion Products in Pressurized Water Reactors*. 1009951